

## Photophysical Properties of TlGaS<sub>2</sub> Layered Single Crystals

I. M. Ashraf

Department of Physics, Faculty of Science (Aswan), South Valley University, Aswan, Egypt

Received: October 7, 2003; In Final Form: February 16, 2004

The photoconductivity (PC) of TlGaS<sub>2</sub> layered single crystals was investigated in the 77–300 K temperature, 1000–2500 lx excitation intensity, 10–25 V applied voltage, and 415–535 nm wavelength ranges. Both the alternating current photoconductivity (ac-PC) and the spectral distribution of the photocurrent were studied at different values of light intensity, applied voltage, and temperature. Dependencies of the carrier lifetime on light intensity, applied voltage, and temperature have been investigated as a result of the ac-PC and direct current photoconductivity (dc-PC) measurements. The temperature dependence of the energy gap width was described as a result of studying the dc-PC. The values of the photoconductivity response time, which are reported from the light intensity dependence of ac-PC, presents that there is a continuous distribution of traps in the energy gap.

### Introduction

Thallium chalcogenides received a great deal of attention because of their optical and electrical properties in view of possible optoelectronic device applications.<sup>1–4</sup> The III–III–VI<sub>2</sub> family of crystals have both layered (e.g., TlGaS<sub>2</sub>, TlGaSe<sub>2</sub>, TlInS<sub>2</sub>) and chain (e.g., TlInSe<sub>2</sub>, TlInTe<sub>2</sub>, TlGaTe<sub>2</sub>) structures. References 5 and 6 showed that the photoluminescence band of TlGaS<sub>2</sub> and TlInS<sub>2</sub> single crystals is due to donor–acceptor recombination. At room temperature, layer-structured thallium chalcogenide crystals belong to the monoclinic system with space group *C2/c*. The crystal lattice consists of alternating two-dimensional layers arranged parallel to the (001) plane. Each successive layer is rotated by a 90° angle with respect to the previous layer.<sup>7</sup> Long-wave optical phonons in these crystals were investigated by infrared reflection and Raman scattering measurements.<sup>8</sup> An investigation of the *T*–*P* phase diagram of TlGaS and TlGaSe crystals between room temperature and 520 K under hydrostatic pressure up to 1.2 GPa was made by Allakhverdiev et al.<sup>9</sup> An investigation of the TlGaS<sub>2</sub> single crystal by TSC (thermally stimulated current) and photoinduced current transient spectroscopy has been reported in ref 10. The TSC spectra of the TlGaS<sub>2</sub> single crystal show four peaks whose activation energies are (a) 0.18, (b) 0.23, (c) 0.36, and (d) 0.66 eV. Peaks a and b are located below the conduction band and peaks c and d are located above the valence band. The TSC spectra show four deep traps whose activation energies are 0.17, 0.23, 0.35, and 0.65 eV.

The aim of this work is to elucidate the photoconductivity (PC) of TlGaS<sub>2</sub> single crystals in different conditions. The resultant actual behaviors of the direct current photoconductivity (dc-PC) and alternating current photoconductivity (ac-PC) spectra for TlGaS<sub>2</sub> are discussed and analyzed. Important physical parameters are estimated and their temperature dependencies are discussed. In the present work, we report the results of the PC investigation of TlGaS<sub>2</sub> single crystals, which has a band gap of  $E_g \approx 2.61$  eV at *T* = 77 K. The PC investigation is conducted in the 514–535 nm wavelength, 1000–2500 lx excitation intensity, 10–25 V applied voltage, and 77–300 K temperature ranges.

### Experimental Details

TlGaS<sub>2</sub> single crystals were synthesized from elements of high purity 99.9999 (Aldrich Mark). The starting materials were weighed individually by an using electronic balance (Startorius Mark) with a sensitivity of 10<sup>–4</sup> g. These starting materials are 6.8123 g of thallium, 2.3249 g of gallium, and 2.1376 g of sulfur. The single crystals of TlGaS<sub>2</sub> were synthesized and grown in evacuated silica ampules by using a method related to the Bridgman technique. Such a silica ampule containing the TlGaS<sub>2</sub> compound was evacuated to 10<sup>–6</sup> Torr and sealed under vacuum. The ampule was placed in a three-zone tube furnace.<sup>11</sup> At the beginning of the growth run, the ampule was held in the first zone at 1160 K. The middle zone corresponds to the crystallization temperature (1059 K).<sup>12</sup> The rate of propagation of crystallization was 0.19 cm/h. In the final stage, the ampule was taken from the third zone at room temperature. The X-ray diffraction data showed that TlGaS<sub>2</sub> crystallizes in a monoclinic unit cell with lattice parameters *a* = 10.40 Å, *b* = 10.40 Å, *c* = 15.17 Å, and  $\beta = 100^\circ$ .<sup>13</sup> The samples were prepared by cleaving an ingot parallel to the crystal layer, which was perpendicular to the *c* axis. In a direction perpendicular to the *c* axis and parallel to the cleavage plane, the photocurrent was measured. The electrical conductivity of the samples was p type as determined by the hot probe method. Then, the sample under study was mounted on the coldfinger inside a cryostat (Oxford DN1704-type), which was evacuated to about 10<sup>–4</sup> Torr. The temperature inside the cryostat was controlled by a digital temperature controller (Oxford ITC601-type). A silver paste was used for making the contact between the specimen and the metal electrodes. The *I*–*V* characteristics of this specimen showed that the conduction is ohmic in the range 0–25 V of applied voltage, at which the PC was studied. Excitation was done by a tungsten lamp (1000 W). The incident light was focused by an optical system consisting of two convex lenses. Then, a homogeneous illumination was obtained. Mechanical choppers (SR540-type) and a valve microvoltmeter (TM3B-type) were used to record the data of the ac-PC measurements. For studying the dc-PC of TlGaS<sub>2</sub>, an electrometer (Keithly 610-type) and a monochromator (Carl Zeiss M4GII-type) were used.

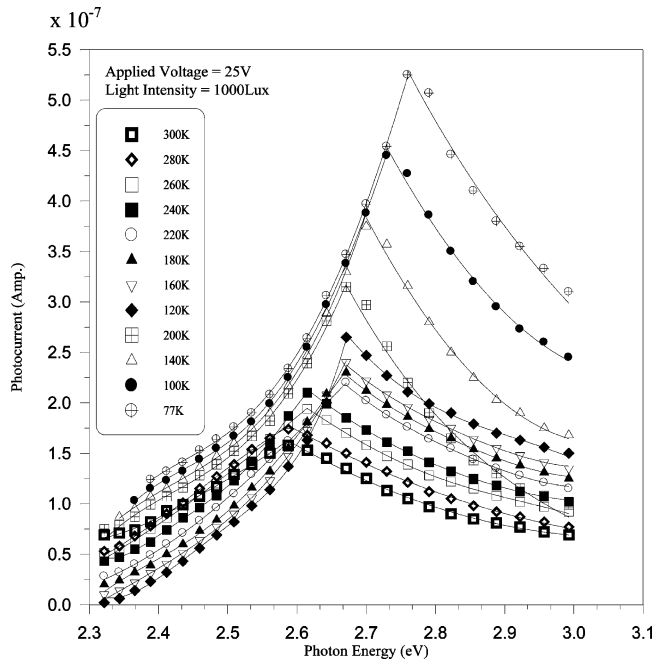


**Figure 1.** Spectral distribution of the dc-PC for TiGaS<sub>2</sub> single crystals in the temperature range 77–300 K.

## Results and Discussion

The high photosensitivity of crystals TiGaS<sub>2</sub> made it possible to study dc-PC spectra in a wide range of the photon energy. Figure 1 presents the spectral distribution of dc-PC for the TiGaS<sub>2</sub> single crystal in the temperature range 77–300 K, in the 415–535 nm wavelength range. Some of the spectra of dc-PC was plotted, which shows that the photocurrent decreases with increasing temperature except at 140 and 200 K, where it has higher values than at 120 K (Figure 1); this could be due to the trapping (capture) process. The dc-PC has one peak in the temperature range 77–300 K, which is associated with direct band–band transition. At 77 K, the peak was found at 2.76 eV, which shifts toward the long wavelength side with increasing temperature.

The spectral sensitivity curve for an intrinsic semiconductor can be the following relation:<sup>14</sup>

$$S(E) = \frac{1}{1 + \exp[B(E_0 - E)]} \quad (1)$$

where  $B$  is constant,  $E$  is the energy at any wavelength, and  $E_0$  is the energy at the threshold wavelength. This curve has a flat response at short wavelengths and an exponential fall with energy at long wavelengths. It is assumed that the varying sensitivity results from the distribution of energy levels from which the photoelectrons originate or to which they go. Busch<sup>15</sup> and Rose<sup>16</sup> have considered such a distribution of centers. If we assume that  $N(E) dE$  represents the number of levels per unit volume lying between  $E$  and  $E + dE$ , then when the material is irradiated by a given quantum energy  $E_\lambda$  the amount of absorption and, hence, the sensitivity will be proportional to the total number of centers of energy lower than  $E_\lambda$ , that is,

$$\int_0^{E_\lambda} N(E) dE \therefore S(E) \approx \int_0^{E_\lambda} N(E) dE$$

which leads to

$$N(E) = G \frac{dS(E)}{dE} \quad (2)$$

where  $G$  is constant. Using eq 1 in eq 2, we obtain

$$N(E) = [GBe^{B(E_0-E)}] / [1 + e^{B(E_0-E)}]^2 \quad (3)$$

From this expression, the number of electrons that will be present in the conduction band as a result of thermal excitation from level  $E$  can be calculated from this distribution of levels to be

$$n = C(G/B)^{1/2} \frac{\pi}{\sin(\pi a)} \exp[-E_0/(2kT)] \quad (4)$$

where  $C$  is a constant and  $G$  means the PC gain, which is defined as the photosensitivity of a photoconductor in terms of the number of charge carriers (the carrier pass between the electrodes per second for each photon absorbed). This definition has been reported in ref. 17. The above relation is similar to that obtained for the Hall effect using a simple theory of electrons excited into the conduction band from one definite energy level:<sup>18</sup>

$$n = n_0 \exp[-E_g/(2kT)] \quad (5)$$

where  $E_g$  is the width of the forbidden gap for intrinsic conductivity.

Hence, by comparison of eq 4 with eq 5 we get  $E_g = E_0$ . Thus, when  $E = E_g$  the sensitivity  $S$  can be described by the following relation

$$S = \frac{1}{1 + \exp(E_0 - E_g)} = \frac{1}{2} \quad (6)$$

This leads to an important conclusion that the activation energy is determined from the spectral curve as the point where the sensitivity has fallen to 1/2 of its value, that is,

$$E_0 = E_g = \text{quantum energy at } \lambda_{1/2} \quad (7)$$

Therefore, knowing  $\lambda_{1/2}$  we can determine the gap width ( $E_g$ ) as

$$E = hv = hc/\lambda_{1/2}$$

Applying the  $\lambda_{1/2}$  method, the energy gap  $E_g$  could be calculated at every temperature as shown in Figure 2, which shows that the values of the energy gap decrease as temperature increases. The temperature coefficient of  $E_g$  ( $dE_g/dT$ ) was calculated from the straight-line portion; it was found to be  $-7.58 \times 10^{-4}$  eV/K. According to eq 8, the sign may be due to that the electron–phonon interaction term is larger than the lattice expansion contribution:<sup>19</sup>

$$dE_g/dT = (dE_g/dT)_{L-ex} + (dE_g/dT)_{e-p} \quad (8)$$

where the first term depends on the lattice expansion and the second term depends on the electron–phonon interaction. Such behavior is typical for crystals having a layered structure.<sup>20</sup> The dependence of  $E_g$  on temperature can describe by the following empirical expression:<sup>21</sup>

$$E_g(T) = E_g(0) - \delta[T^2/(T + \beta)] \quad (9)$$

where  $E_g(0)$  is the energy gap at 0 K and  $\delta$  and  $\beta$  are constants.

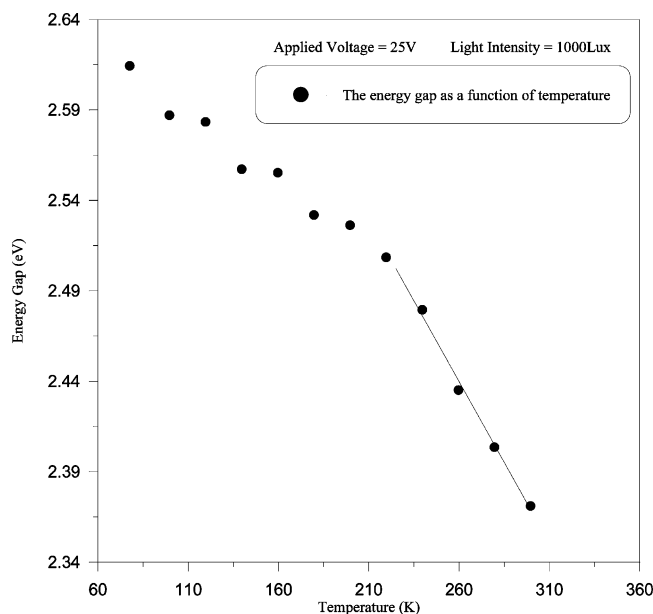


**Figure 2.** Energy gap versus temperature plotted from the dc-PC results.

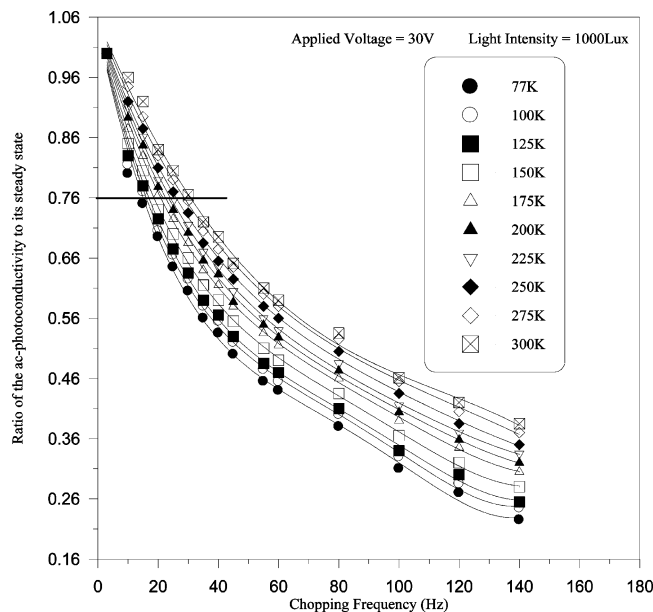


**Figure 3.** Frequency dependence of ac-PC for TiGaS<sub>2</sub> single crystals in the temperature range 77–300 K.

Frequency dependence measurements of the ac-PC for TiGaS<sub>2</sub> single crystals were carried out to study their kinetics.  $\Delta\sigma_{\sim}(F)/\Delta\sigma_{st}$  is plotted as a function of  $F$  (see eq 10), where  $\Delta\sigma_{\sim}$  is the ac component of the ac-PC,  $\Delta\sigma_{st}$  presents its steady state, and  $F$  is the chopping frequency. Figure 3 presents the frequency dependence of ac-PC of the TiGaS<sub>2</sub> single crystal in the temperature range 77–300 K. The behaviors of the curves in all temperature ranges under study are similar and have a general shape. The ac-PC decreases by increasing the frequency in the whole range of investigated frequencies. Both the frequency dependencies of ac-PC at different values of applied voltage and light intensity were shown in Figures 4 and 5. The first decay regions in Figures 3–5 may be controlled by band-to-band recombination depending on the lifetime of the majority carriers (holes in the material under study).<sup>22</sup> The slow decay regions are believed to be due to extrinsic transition.<sup>16</sup>

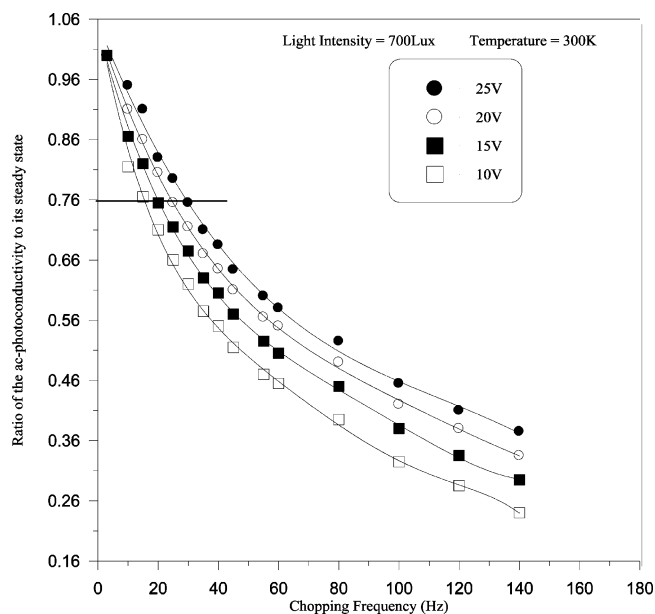


**Figure 4.** Frequency dependence of ac-PC for TiGaS<sub>2</sub> single crystals at different values of applied voltage.

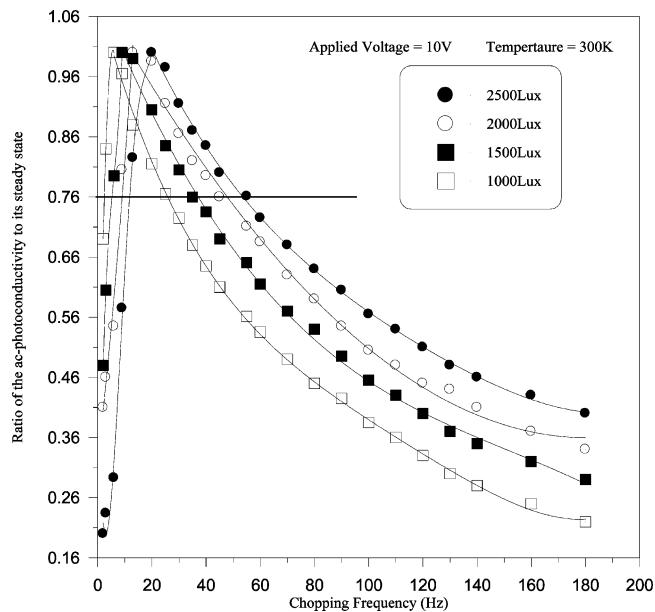


**Figure 5.** Frequency dependence of ac-PC for TiGaS<sub>2</sub> single crystals at different values of light intensity.

The lifetime of the charge carriers can be evaluated for each temperature, applied voltage, and light intensity by using this relation:<sup>18</sup>

$$\frac{\Delta\sigma_{\sim}(F)}{\Delta\sigma_{st}} = \tanh\left(\frac{1}{4F\tau}\right) \quad (10)$$

where  $\tau$  refers to the carrier lifetime. This can be done by drawing a straight line parallel to the frequency axis at a height of 0.76 from the maximum (where  $\tanh 1 = 0.76$ ) and a normal drops from the point of intersection on the frequency axis to cut off a segment equal to  $1/4\tau$  from the frequency axis.

The effect of temperature on the carrier lifetime is described in Figure 6. The lifetime decreases with increasing the temperature in the range 77–300 K. Decreasing of the carrier lifetime with increasing temperature is attributed to more trapping in the recombination centers. The effects of applied voltage and

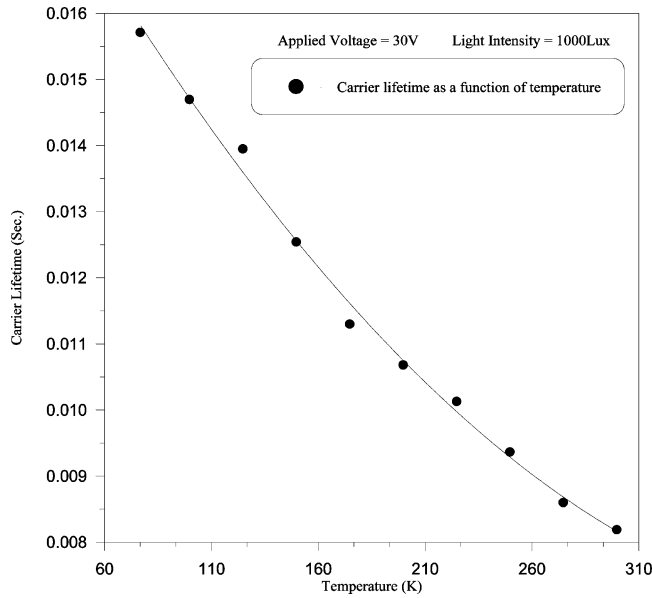


**Figure 6.** Temperature dependence of lifetime for TI GaS<sub>2</sub> single crystals.

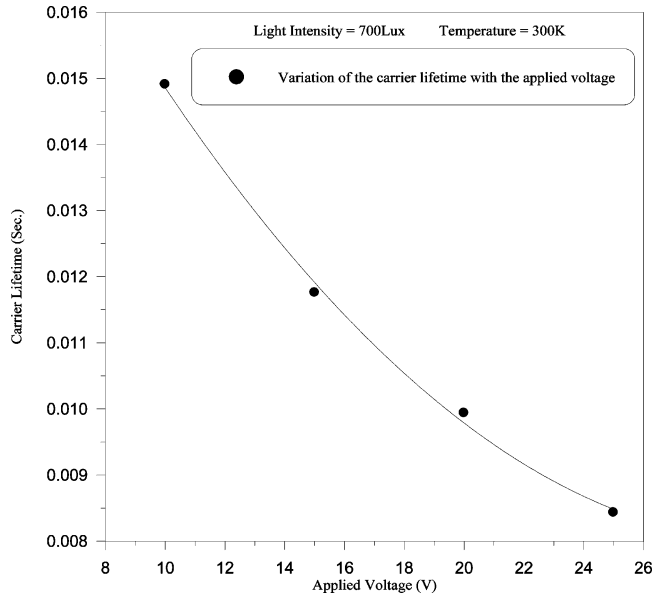


**Figure 7.** Applied voltage dependence of lifetime for TI GaS<sub>2</sub> single crystals.

light intensity on the carrier lifetime were presented graphically in Figures 7 and 8. Figure 7 shows that the lifetime decreases with increasing the applied voltage, which could be due to the trapping process and increasing of carrier velocity according to the relation

$$\tau = (vsN)^{-1} \quad (11)$$

where  $v$  is the carrier velocity,  $s$  is the capture cross section, and  $N$  is the carrier concentration. The value of the lifetime decreases with increasing the light intensity (Figure 8), which could be due to that the probability of trapping increases with increasing the intensity of the exciting light. Variation of ac-PC with light modulation frequency for different light intensities is shown in Figure 5. The ac-PC in the plot is normalized with respect to its maximum value. The photoconductivity response time (PRT) is calculated using the relation  $\tau = 1/(2\pi F_{\max})$ , where  $F_{\max}$  is the frequency at which ac-PC shows a peak in its value.<sup>23</sup> From the frequency dependence of ac-PC at different

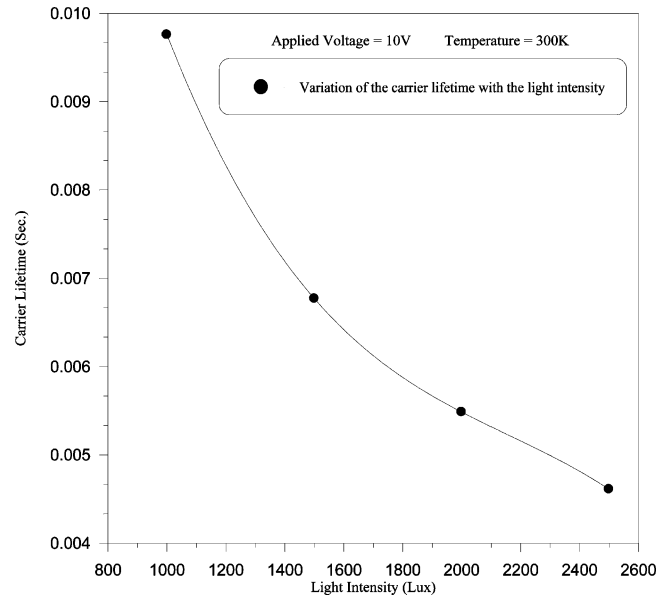


**Figure 8.** Light intensity dependence of lifetime for TI GaS<sub>2</sub> single crystals.

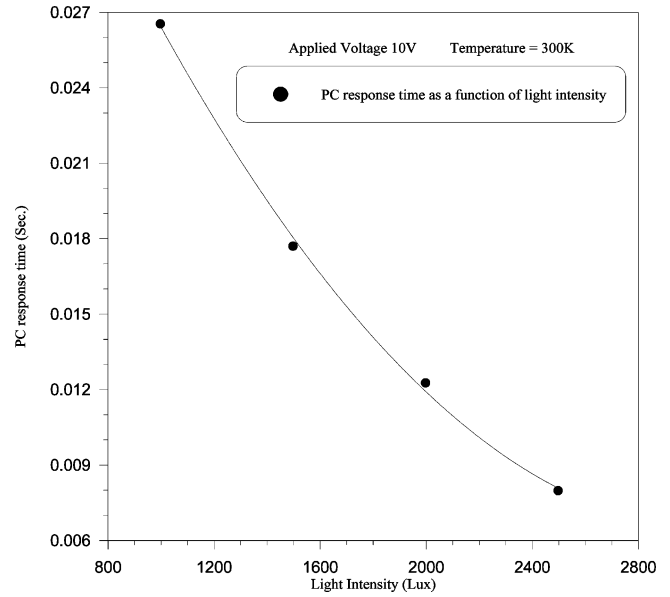


**Figure 9.** Light intensity dependence of the PRT for TI GaS<sub>2</sub> single crystals.

light intensities, it is found that the position of  $F_{\max}$  shifts toward higher frequencies with increasing the light intensity (Figure 9). These frequency dependencies of ac-PC show that the PRT decreases with increase in light intensity. Because the light intensity is directly proportional to the carrier generation rate ( $g$ ), the PRT ( $\tau$ ) and  $g$  can be related by the expression<sup>23–25</sup>

$$\tau = Ag^{\nu} \quad (12)$$

Variation of  $\ln(\tau)$  with  $\ln(g)$  has been plotted, and from the slope of the straight line graph so obtained, the value of the exponent  $\nu$  has been calculated. The value of  $\nu$  at different light intensities lies between 0.5 and 1. A value of  $\nu$  lying between 0.54 and 1 is an indication for a continuous distribution of traps in the energy gap.<sup>26</sup>

## Conclusion

The dc-PC spectra have one peak for the entire range of temperatures (77–300 K); its position in the energy gap is found

at 2.76 eV at 77 K. The photoppeak shifts toward the long wavelength side with increasing temperature. The spectral distribution of the dc-PC shows that the photocurrent shifts toward its higher values as the light intensity and applied bias voltage increase with the same behaviors. It was calculated that TiGaS<sub>2</sub> has a band gap  $E_g = 2.61$  eV at 77 K and takes low values as the temperature increases with the temperature coefficient  $dE_g/dT = -7.58 \times 10^{-4}$  eV/K. The ac-PC data lead to that the carrier lifetime decreases with increasing of temperature in the range 77–300 K. This decrease could be due to the increase in the trap centers. High values of both the applied voltage and the light intensity reduce the value of the carrier lifetime, which could be due to the increase in the carrier velocity and in the trap centers. The relation between  $\ln(\tau)$  and  $\ln(g)$  shows that the exponent  $\nu$  lies between 0.54 and 1, which is an indication for a continuous distribution of traps in the energy gap.<sup>26</sup>

**Acknowledgment.** The author is much indebted to Prof. Dr. A. E. Belal [Physics Department, Faculty of Science (Aswan), South Valley University, Egypt] for his help and encouragement.

## References and Notes

- (1) Yee, K. A.; Albright, A. *J. Am. Chem. Soc.* **1991**, *113*, 6474.
- (2) Halias, M. P.; Anagnostopoulos, A. N.; Kambas, K.; Spyridelis, J. *Mater. Res. Bull.* **1992**, *27*, 25.
- (3) Kalkan, N.; Kalomiros, J. A.; Halias, M.; Anagnostopoulos, A. N. *Solid State Commun.* **1996**, *99*, 375.
- (4) Kalomiros, J. A.; Kalkan, N.; Halias, M.; Anagnostopoulos, A. N.; Kambas, K. *Solid State Commun.* **1995**, *96*, 601.
- (5) Gasanly, N. M.; Aydinli, A.; Bek, A.; Yilmaz, I. *Solid State Commun.* **1998**, *105*, 21.
- (6) Aydinli, A.; Gasanly, N. M.; Yilmaz, I.; Serpenguzel, A. *Semicond. Sci. Technol.* **1999**, *14*, 599.
- (7) Gasanly, N. M.; Serpenguzel, A.; Aydinli, A.; Baten, S. M. A. *J. Lumin.* **2000**, *86*, 39.
- (8) Gasanly, N. M.; Goncharov, A. F.; Melnik, N. N.; Ragimov, A. S.; Tagirov, V. I. *Phys. Status Solidi B* **1983**, *116*, 427.
- (9) Allahverdiev, K. R.; Mamedov, T. G.; Peresada, G. I.; Ponyatovskil, E. G.; Sharifov, Ya. N. *Sov. Phys. Solid State* **1985**, *27*, 3.
- (10) Song, H.-J.; Yun, S.-H.; Kim, W.-T. *Solid State Commun.* **1995**, *94*, 3.
- (11) Hussein, S. A.; Nagat, A. T. *Cryst. Res. Technol.* **1989**, *24*, 283.
- (12) Guseinov, G. D.; Ramazade, A. M.; Kerimova, E. M. *Phys. Status Solidi* **1967**, *22*, K117.
- (13) Muller, D.; Poltmann, F. E.; Hahn, H. Z. *Naturforsch* **1974**, *296*, 117.
- (14) Moss, T. S. *Photoconductivity in Elements*; Butterworths: London 1952.
- (15) Busch, G. *Phys. Acta* **1946**, *19*, 198, 32.
- (16) Rose, A. C. *RCA Rev.* **1951**, *12*, 362, 32, 40.
- (17) Bube, R. *Photoconductivity of solids*; Wiley: New York, 1960.
- (18) Ryvkin, S. H. *Photoelectric Effects in Semiconductors*; Consultants Bureau: New York, 1964.
- (19) Gurbulak, B. *Appl. Phys.* **1999**, *A58*, 353–356.
- (20) Halias, M.; Anagnostopoulos, A.; Kambas, K.; Spyridelis, S. *Physica B* **1989**, *160*, 154.
- (21) Varshni, V. P. *Physica* **1967**, *34*, 149.
- (22) Raturai, A. K.; Thangaraj, R.; Raja, P. R.; Tripathi, B. B.; Agnihotri, O. P. *Thin Solid Films* **1983**, *106*, 257.
- (23) Kaplan, R. *J. Phys.: Condens. Matter* **1995**, *7*, 6847.
- (24) Bullo, J.; Cordier, P.; Gouthier, M.; Mawawa, G. *Philos. Mag.* **1987**, *B55*, 599.
- (25) Searle, T. M. *Philos. Mag. Lett.* **1990**, *61*, 251.
- (26) Mathew, G.; Philip, J. *Pramana* **1999**, *53*, 5.